https://dx.doi.org/10.1016/j.istruc.2018.11.015
This is the Pre-Published Version.

Recent research advances of high strength steel welded hollow section joints

Xiaoyi Lan, Tak-Ming Chan*

Dept. of Civil and Environmental Engineering, The Hong Kong Polytechnic University, Hung Hom, Hong Kong, China
*tak-ming.chan@polyu.edu.hk

Abstract: High strength steel (HSS) with acceptable toughness and ductility has been produced due to advances in steel manufacturing technologies. The application of HSS in tubular structures could significantly reduce construction costs and lower carbon footprints. Welded hollow section joints are critical components in tubular structures. This paper aims to provide a review of recent research advances of HSS welded hollow sections joints. Current design rules and their research background for welded hollow section joints under static and fatigue loadings are firstly described. Recent investigations on the static design and fatigue performance of HSS welded hollow section joints are summarised, and further research work is discussed. The preliminary results indicate that suitability of current design rules for the HSS welded joints under static loading depends on the loading type, failure mode, steel yield stress, geometric parameters, chord preload ratio and welding. High-cycle fatigue performance of the HSS welded joints is comparable or even higher when compared with normal strength steel counterparts. More research is highly desirable for comprehensive assessment of current design provisions and proposing appropriate design rules for the HSS welded joints.

Keywords: Rectangular hollow section; Circular hollow section; Welded joints; High strength steel; Static design; High-cycle fatigue; Low-cycle fatigue

1. Introduction

High strength steel (HSS) with yield stresses higher than 450 MPa becomes readily available because of rapid development of steel production technologies such as quenching and tempering (QT) and thermo-mechanical controlled processing (TMCP). The QT technique was firstly developed in the 1960s to manufacture HSS of steel grade S690 [1]. The steel is rapidly cooled down after austenizing at about 900°C in a metallurgical process of quenching, in order to introduce a hard form of crystalline structure of martensite. Targeted high steel yield strengths can be obtained in the quenching treatment. Tempering is, thereafter, performed to reheat the steel at around 600°C in order to improve toughness and ductility of HSS. Thermo-mechanical controlled processing (TMCP) is another main means to produce HSS with finer grain microstructures. The TMCP technique applies a controlled rolling at a lower temperature about 700°C and a subsequent accelerated cooling process. The use of alloying elements is also minimised involving optimized microalloying in each manufacturing stage. Thus, the energy consumption and carbon equivalent value (CEV) of TMCP steel are lower, and the weldability is improved when compared with traditional QT steel [2]. It is also worth noting that high-purity steelmaking technologies developed in recent years such as hot metal dephosphorization processes could significantly improve steel purity [3]. Contents of impurity elements e.g. phosphorus and sulphur which adversely affect steel toughness are reduced, and therefore the steel toughness and ductility are improved. This technique in conjunction with the QT or TMCP technologies can produce HSS with acceptable toughness and ductility nowadays.

Fig. 1 shows typical buildings and bridges in which HSS has been successfully used [4, 5]. The

© 2018. This manuscript version is made available under the CC-BY-NC-ND 4.0 license http://creativecommons.org/licenses/by-nc-nd/4.0/

application of HSS with high strength-to-weight ratio can reduce member sizes and structural self-weight, resulting in material savings, reduced costs of transportation, coatings and foundations, and thus lower construction costs. Carbon footprints are also reduced because of less resource consumption and transportation time. Recognising the benefits of HSS as an economical and sustainable construction material, it is increasingly popular in construction industry. Tubular structures are widely used in onshore and offshore structures e.g. buildings, large-span roofs, bridges and offshore platforms. HSS welded hollow section joints composed of built-up, hot-finished or cold-formed steel tubes are critical components in tubular structures. Built-up hollow sections welded from HSS steel plates are preferred in the case of heavy loadings while hot-finished and cold-formed steel hollow sections are usually adopted in light tubular structures. It should be noted that material properties of HSS differ from those of normal strength steel. There are usually no sharply defined yield points in stress-strain responses of cold-formed HSS, and thus the 0.2% proof stresses are then taken as the yield stresses. Deformation capacity and ductility of HSS are generally lower for the trade-off of higher material strengths, and the yield ratio of yield to ultimate stresses is closer to unity when compared with normal strength steel. Extensive investigations have been conducted on material properties of HSS [5-8]. Structural performance of HSS welded hollow section joints could differ from that of normal strength steel counterparts. Comprehensive research on the HSS welded joints is therefore highly desirable in order to propose suitable design rules for the joints and to facilitate the application of HSS tubular structures.

Structural behaviours of welded hollow section joints using normal strength steel have been extensively investigated. In contrast, research on the HSS welded joints remains limited. Design rules for welded hollow section joints using steel grades up to S700 are available in international design guides and codes. This paper firstly describes the current design rules and their research background for normal and high strength steel welded hollow section joints under static and fatigue loadings. Recent research advances of static design and fatigue performance of the HSS welded joints are summarised. Suitability of the current design rules and research needs for the HSS welded joints are discussed.

2. Current design rules for welded hollow sections joints

2.1. Static design

The International Institute of Welding (IIW) Subcommission XV-E proposed the 1st edition of design recommendations [9] in 1981, and later developed the 2nd edition in 1989 [10] and the 3rd edition in 2009 [11] for welded hollow section joints under predominantly static loading. The Eurocode EN 1993-1-8 [12] and ANSI/AISC 360-10 [13] generally follow the 2nd edition of IIW recommendations [10]. The 3rd edition of IIW recommendations was adopted by the current CIDECT design guides No. 1 and 3 [14, 15] and ISO 14346 [16]. Design equations for welded CHS joints mainly used in offshore structures are also available in API RP 2A WSD [17]. Strength equations, which are user-friendly, reasonably accurate and consistent among various types of hot-finished and cold-formed steel hollow section joints (see Fig. 2), are specified in these design codes and guides [9-17]. For example, the strength equation for axially loaded uniplanar welded hollow section joints which fail by chord plastification is as follows:

$$N_1^* = \frac{f_y t^2}{\sin\theta} Q_u Q_f \tag{1}$$

The moment resistance of circular hollow section (CHS) joints subjected to in-plane and out-of-plane bending in the brace is as follows:

$$M_1^* = \frac{f_y t^2}{\sin\theta} Q_u Q_f d_1 \tag{2}$$

The moment capacity of rectangular hollow section (RHS) joints under in-plane bending ($M^*_{ip,1}$) and out-of-plane bending ($M^*_{op,1}$) in the brace is as follows:

$$M_{ip,1}^* = \frac{f_y t^2}{\sin\theta} Q_u Q_f h_1 \tag{3}$$

$$M_{op,1}^* = \frac{f_y t^2}{\sin\theta} Q_u Q_f b_1 \tag{4}$$

where f_y is the yield stress of the chord member, t is the chord wall thickness, θ is the angle between the brace and chord, d_1 is the brace diameter, h_1 is brace height, b_1 is the brace width, Q_u is the reference strength equation expressed as a function of non-dimensional joint geometric parameters, and the chord stress equation (Q_f) accounts for the effect of chord longitudinal stresses on the joint strength. The reference strength equations (Q_u) adopted for CHS X-joints are based on the ring model, and the yield line model is employed to derive the reference strength equations for RHS T-, Y- and X-joints [10-16]. These analytical models for welded hollow section joints are elaborated in Wardenier [18].

Different definitions of the static strength of welded hollow section joints were adopted in the development of design rules. In the early research on welded hollow section joints, the ultimate load was taken as the joint strength. This definition was employed in the 2nd edition of IIW recommendations [10], EN 1993-1-8 [12] and ANSI/AISC 360-10 [13]. However, some hollow section joints do not exhibit peak loads in load-deformation curves due to the membrane effect and strain hardening of steel materials. Lu et al. [19] proposed an ultimate deformation limit i.e. 3% of chord diameter ($0.03d$) for CHS joints and 3% of chord width ($0.03b$) for RHS joints. Such limit is based on the observation that the deformation at the peak loads of welded hollow section joints ranges from 2.5% to 4% of chord diameter or chord width. It is suggested that the joint strength is determined by the lower of the ultimate load of the hollow section joints and the load at the ultimate deformation limit. This proposal was later adopted by the 3rd edition of IIW recommendations [11], CIDECT design guides No. 1 and 3 [14, 15] and ISO 14346 [16]. The deformation limit serves to control joint deformations at ultimate and serviceability limit states because of high flexibility of some hollow section joints [14, 15]. API RP 2A WSD [17] adopts the Yura deformation limit of $\delta=60d_1f_y/E$ and rotation limit of $\varphi=80f_y/E$ for CHS joints under axial loading and bending, respectively [20]. The δ and φ are the limiting brace end displacement and rotation, respectively, d_1 is the brace diameter, and f_y and E are the steel yield stress and elastic modulus of the chord, respectively.

The strength equations (Eqs. (1) to (4)) adopted in 2nd edition of IIW recommendations [10], EN 1993-1-8 [12] and ANSI/AISC 360-10 [13] for welded hollow section joints were obtained primarily based on test results. In contrast, the 3rd edition of IIW recommendations [11], CIDECT design guides No. 1 and 3 [14, 15] and ISO 14346 [16] are mainly based on FE database because test data inevitably include a certain amount of scatter while FE results could avoid such scatter [21]. The strength equations in API RP 2A WSD [17] are developed from regression analysis using the MSL screened test database, the unscreened test database compiled by Kumamoto University and the API/EWI validated FE database [20]. Comparison among the 2nd and 3rd editions of the IIW recommendations [10, 11] and API RP 2A WSD [17] is made in the appendix of the CIDECT design guides No. 1 and 3 [14, 15]. The major changes in the 3rd edition of the IIW recommendations [11] compared with the 2nd edition [10] and corresponding research background are introduced in Zhao et al. [22].

The IIW recommendations [10, 11], EN 1993-1-8 [12], the CIDECT design guides [14, 15] and ISO 14346 [16] give design strengths for welded hollow section joints. In contrast, the strength equations specified in ANSI/AISC 360-10 [13] and API RP 2A WSD [17] produce characteristic strengths for the joints. The regression analysis of test or numerical data for the reference strength equation (Q_u) and the chord stress equation (Q_f) leads to the mean strength equation. The mean strength equation can be converted to the characteristic strength equation by considering fabrication tolerances, mean values and scatter of test or numerical data and a correction of steel yield stress [21]. When adopted theoretical models e.g. the yield line model for RHS T-, Y- and X-joints produce lower-bound strength predictions for test strengths, the analytical equations derived from the theoretical models could be taken as the characteristic strength equations [23]. The design strength equation can be derived from the characteristic strength equation divided by a partial factor. The partial factors adopted by the design codes and guides [10-12, 14-16] are detailed in Wardenier [23] and Table C.1 of ISO 14346 [16]. The procedures of converting mean strengths to characteristic strengths and then to design strengths adopted by the IIW recommendations [10, 11] are described in van der Vegte et al. [21] and Wardenier [23]. It should be noted that the uniplanar welded hollow section joints which fail by other failure modes e.g. chord punching shear, chord side wall failure, chord shear and local failure of the brace member, welded plate to CHS or RHS chord joints and multiplanar welded hollow section joints are also covered in the design codes and guides [9-17].

Limitations on materials and validity ranges of joint parameters are specified in the design codes and guides [9-17] which are mainly for welded hollow section joints using steel grades up to S355. EN 1993-1-8 [12] and the CIDECT design guides [14, 15] allow for use of steel grades beyond S355, but stipulate restrictive design rules. Additional reduction factors of joint strength are specified to be applied to the design strength equations of welded hollow section joints using normal strength steel. EN 1993-1-8 [12] prescribes a reduction factor of 0.9 for the welded joints using steel grades greater than S355 and up to S460. EN 1993-1-12 [24] further extends the limit of steel grades beyond S460 and up to S700, and imposes a reduction factor of 0.8. Similarly, the CIDECT design guides [14, 15] stipulate a reduction factor of 0.9 and specify the limitation on the yield stress (f_y) to 0.8 of the ultimate stress (f_u) for the welded joints using steel grades greater than S355 and up to S460. These restrictions are imposed for the welded joints in steel grades greater than S355 due to relatively larger deformation for chord face plastification, possibly lower deformation and rotation capacity, and required sufficient connection ductility for chord punching shear and local yielding of braces [14, 15].

The restrictive design rules aforementioned for the welded joints using steel grades beyond S355 are mainly based on limited investigations on gap K-joints. Liu and Wardenier [25] numerically analysed the static strength of RHS gap K-joints using S460 steel and found that the joint strength is 10 to 16% lower than that of corresponding S235 joints in relative terms. Kurobane [26] conducted experimental tests on CHS gap K-joints in S460 steel and found that the joint strength is 18% lower when compared with the same joints using S235 steel. Noordhoek et al. [27] also reported similar findings that the joint efficiency of CHS gap K-joints in S460 steel is lower than that of corresponding S235 joints. In recent years, some investigations re-evaluated the design rules for HSS welded hollow section joints under static loading, which will be discussed in Section 3.

2.2. Fatigue design

Numerous tubular structures are under fatigue loading e.g. offshore platforms subjected to time-variant impact from ocean waves. Fatigue loading could lead to initiation of cracks, subsequent crack growth and progressive strength degradation. Fracture of members or welded hollow section joints could eventually occur, which may result in the collapse of tubular structures. Phases of crack initiation and crack propagation are two major parts of the fatigue life. The joint type, applied loading and structural detailing are three controlling factors of fatigue resistance for welded hollow section joints i.e. the number of cycles to fatigue failure (N_f).

The IIW Subcommission XV-E proposed design recommendations for welded hollow section joints subjected to high-cycle fatigue ($N_f \geq 10^4$) [28] which form the basis of the CIDECT design guide No. 8 [29]. The hot spot stress method is the most commonly used approach for estimating high-cycle fatigue resistance of welded hollow section joints which is adopted by the CIDECT design guide No. 8 [29]. The non-uniform stiffness in the brace-chord intersection region results in uneven geometric stress distribution. The cracks usually initiate at the hot spot locations where the maximum geometric stress called hot spot stress occurs. For welded hollow section joints, cracking usually takes place at the weld toe. The hot spot stress method which is also named geometric stress method relates the fatigue resistance of welded hollow section joints to the hot spot stress at the weld toe. This method considers the non-uniform stress distribution at the brace-chord intersection directly and effects of the geometry and loading type, but excludes influences related to the fabrication and local condition at the weld toe.

The fatigue resistance of welded hollow section joints can be determined by fatigue strength curves i.e. S_{rhs}-N_f curves, where S_{rhs} is the hot spot stress range and N_f is the number of cycles to fatigue failure. The hot spot stress range can be determined by experimental tests or numerical simulations, which are, however, not readily feasible for designers. In order to facilitate the calculation of the hot spot stress range, the stress concentration factor (SCF) is used as the multiplication factor on the nominal stress range in the member resulted from the applied basic member loading which causes the hot spot stress [29]. The SCF defined as the ratio of hot spot stress to the nominal stress varies around the perimeter at the brace-chord intersection. Several hot spot locations are therefore chosen for a joint, along which the SCF is determined. For example, the hot spot locations for RHS X- and T-joints are shown in Fig. 3.

The SCF can be determined using specially designed strip strain gauges or finite element analysis. Strain perpendicular to the weld toe recommended by the CIDECT design guide No. 8 [29] can be firstly obtained from strain gauges in the so-called extrapolation region where effects of the local weld toe geometry is negligible. The maximum strain at the weld toe (ε_{Max}) is then calculated using linear extrapolation method for CHS joints and the quadratic extrapolation method for RHS joints [29]. The extrapolation method and region are illustrated in Fig. 4. It should be noted that t is the smaller tube wall thickness between the brace and chord. The strain concentration factors for RHS joints ($\mathrm{SNCF_{RHS}}$) and CHS joints ($\mathrm{SNCF_{CHS}}$) are as follows [29]:

$$\mathrm{SNCF_{RHS}} = \varepsilon_{\mathrm{Max}} / (\varepsilon_{\mathrm{AX}} + \varepsilon_{\mathrm{IPB}} + \varepsilon_{\mathrm{OPB}}) \tag{5}$$

$$\mathrm{SNCF_{CHS}} = \varepsilon_{\mathrm{Max}} / (\varepsilon_{\mathrm{AX}} + \sqrt{\varepsilon_{\mathrm{IPB}}^2 + \varepsilon_{\mathrm{OPB}}^2}) \tag{6}$$

where ε_{Max} is the extrapolated maximum strain, ε_{AX}, ε_{IPB} and ε_{OPB} are the nominal strain caused by the axial force, in-plane bending and out-of-plane bending, respectively. The SCF values of RHS joints ($\mathrm{SCF_{RHS}}$) and CHS joints ($\mathrm{SCF_{CHS}}$) can be obtained by [29]:

$$\mathrm{SCF_{RHS}} = 1.1\mathrm{SNCF_{RHS}} \tag{7}$$

$$\mathrm{SCF_{CHS}} = 1.2\mathrm{SNCF_{CHS}} \tag{8}$$

SCF formulae for the hot spot locations of T-, Y-, X-, K-, XX- and KK-joints composed of RHS and CHS steel tubes obtained from regression analysis of test and numerical results are available in the CIDECT design guide No. 8 [29].

It should be noted that the fatigue strength curves specified in the CIDECT design guide No. 8 [29] are only applicable for welded CHS and RHS joints with tube wall thickness (t) of 4 mm and larger. The test data used for the development of the fatigue design rules for welded hollow section joints are mostly from the welded joints composed of hot-rolled thick-walled tubes using normal strength steel [30]. Extrapolating the existing fatigue strength (S_{rhs}-N_f) curves for thin-walled welded joints (t<4mm) could produce unconservative prediction of fatigue resistance, possibly because of the effect of weld defects [31]. Additionally, applicability of such design rules for high strength steel counterparts in built-up, cold-formed and hot-finished steel sections needs to be examined. Related recent research advances will be summarised in Section 4.

3. Research advances of HSS welded hollow section joints under static loading

3.1. General

The restrictive provisions for HSS welded hollow section joints described in Section 2.1 partially eliminate the benefits of using HSS. The reduction factors of joint strength are imposed for all types of HSS welded hollow section joints regardless of failure modes. Suitability of such design rules remains controversial. In recent years, experimental and numerical studies on HSS welded hollow section joints have been carried out to re-evaluate these design rules. The following subsections summarise recent research advances of HSS welded rectangular hollow section (RHS) and circular hollow section (CHS) joints under static loading and discuss research needs.

3.2. Welded RHS joints

The structural behaviour and static strength of axially loaded welded RHS joints in C450 steel with a nominal yield stress of 450 MPa have been investigated. Becque and Wilkinson [32] reported an experimental program consisting of 4 T-joints and 11 X-joints fabricated from cold-formed C450 steel RHS tubes. Axial compression or tension was applied in the braces. Chord face plastification, chord side wall failure, chord punching shear and local failure of braces were observed in tests. Test strengths of the joints were compared with nominal strengths of the CIDECT design guide [15]. The nominal strengths were converted from the CIDECT design strengths by multiplying the implicit safety factors incorporated in the CIDECT design equations and without applying the specified reduction factor and limitation on the yield stress. It is found that the test strengths exceed the CIDECT nominal strengths for the joints which failed by ductile modes of chord face plastification and chord side wall failure, provided that the joint parameters are within the validity ranges of the CIDECT design equations. The nominal strength prediction becomes increasingly conservative with increasing chord side wall slenderness for the joints which failed by chord side wall failure. The test program, however, provides test evidence justifying the application of the reduction factor and limitation on yield stress for the joints which failed by less ductile modes of chord punching shear and effective width failure of braces. It is also suggested that the current CIDECT design rules should not be applied to the joints with geometric parameters falling outside the CIDECT validity ranges. Cheng and Becque [33] proposed a design methodology for chord side wall failure in axially compressed equal-width RHS X-joints using C450 steel which can consider the effect of compressive chord preload. Mohan et al. [34, 35] numerically analysed the static strength of RHS T-, X-, K- and

N-joints in C450 steel and found that the numerical strengths are generally higher than the CIDECT design strengths without applying the reduction factor and limitation on yield stress.

For higher steel grades not greater than S700, Kim [36] conducted tests on RHS X-joints with a nominal yield stress of 650 MPa and found that the joint strength obtained from tests exceeds the design strength calculated from EN 1993-1-8 [12] without applying reduction factors. Strength equations for chord side wall failure in equal-width RHS X-joints were proposed. Havula et al. [37] carried out tests on S420, S500 and S700 steel square hollow section (SHS) T-joints subjected to in-plane bending to investigate the moment resistance, rotation stiffness and ductility of the T-joints. Chord face plastification governed the deformation of specimens and punching shear eventually occurred in the heat affected zone (HAZ). It is found that the test strengths of butt-welded T-joints and the S700 steel T-joints with small fillet welds are lower than the design strengths predicted by EN 1993-1-8 [12] without using the reduction factors. However, the test strengths of the T-joints using large fillet welds and the S420 and S500 steel T-joints using small fillet welds are higher than the Eurocode design strengths without using the reduction factors. The moment resistance and rotation stiffness of fillet-welded T-joints increase with increasing weld size and are generally higher than those of butt-welded joints. Ductility of the T-joint specimens is found to be sufficient.

Welded RHS joints in ultra-high steel grade of S960 were also investigated in some experimental programs. Feldmann et al. [38] carried out experimental tests on totally 106 RHS X- and K-joints using S500, S700 and S960 steel to evaluate suitability of the reduction factors and throat thickness of fillet welds stipulated in EN 1993-1-8 [12] and 1993-1-12 [24]. Chord plastification, chord side wall failure, chord punching shear, chord shear and weld failure were reported in tests. The maximum loads obtained from tests without considering deformation limits were compared with the Eurocode design strengths without and with applying the reduction factors. It is found that the ultimate loads generally exceed the design strengths using the reduction factors, and the throat thickness calculated from EN 1993-1-8 [12] is conservative. It is suggested that the reduction factors can be relaxed i.e. 1.0, 0.9 and 0.8 for steel grades S500, S700 and S960, respectively. When the weld design is based on the joint strength, the recommended throat thickness is $1.0t$, $1.2t$ and $1.4t$ for steel grades S500, S700 and S960, respectively, where t is the smaller tube wall thickness between the brace and chord. It is noted that the test data are relatively scattered, and such suggestions are based on the lower bound of test strengths. Pandey and Young [39] conducted experimental tests on RHS X-joints composed of cold-formed S960 steel tubes under axial compression in the braces. The tested specimens failed by chord face plastification, chord side wall failure and a combination of the two failure modes. The test strengths were compared with design strengths calculated from EN 1993-1-8 [12] and the CIDECT design guide [15] without using the stipulated reduction factors. It is found that the design equations are unconservative for RHS X-joints with small brace to chord width ratio and become increasingly conservative with increasing chord side wall slenderness for equal-width RHS X-joints.

3.3. Welded CHS joints

Structural performance of HSS welded CHS X-joints has been extensively investigated. Puthli et al. [40] conducted numerical simulations on S460 and S690 steel CHS X-joints and experimental tests on CHS X-joints in steel grades S460, S690 and S770. Axial compression, tension or in-plane bending was applied in the brace. The numerical analysis shows that the reduction factors of joint strength obtained from numerical simulations are higher than 0.9 for the S460 joints and larger than 0.8 for the S690 joints which failed by chord face plastification. Failure modes in tests are chord face plastification and chord punching shear. The test results show that the static strength of the joints under axial tension is considerably higher than that of the joints subjected to axial compression. The test strengths are generally higher than the design strengths calculated from EN 1993-1-8 [12] without applying the reduction factors. Lee et al. [41] carried out test and numerical investigations on CHS X-joints with a nominal yield stress of 650 MPa, which failed by chord plastification. It is also found that test and numerical joint strengths exceed design strengths of EN 1993-1-8 [12] without applying the reduction factors, and the joints appear to have acceptable ductility and deformation capacity. Lan et al. [42] conducted numerical analysis on the static strength of axially compressed CHS X-joints in S700, S900 and S1100 steel which failed by chord plastification. Test data of CHS X-joints with nominal yield stresses of 650, 690 and 770 MPa in the literature were also compiled. The obtained numerical and test strengths were compared with those calculated from mean strength equations on which design equations in EN 1993-1-8 [12] and the CIDECT design guide [14] are based. It is found that suitability of the mean strength equations for HSS CHS X-joints depends on steel yield stress, brace to chord diameter ratio, chord diameter to wall thickness ratio and compressive chord preload ratio. Later, Lan et al. [43] carried out comprehensive analysis on the structural behaviour and static strength of CHS X-joints using steel grades ranging from S460 to S1100 which failed by chord plastification. It is found that effects of heat affected zones (HAZ) on the initial stiffness and static strength of the CHS X-joints could be minor, and the improved yield stresses of HSS generally could not be fully utilised mainly due to the adopted CIDECT deformation limit described in Section 2.1. It is suggested that the chord diameter to wall thickness ratio should be within 40 for steel grades up to S700 and 30 for higher steel grades up to S1100 to allow for more effective use of HSS. Mean and design strength equations were proposed for the CHS X-joints.

HSS welded plate to CHS chord joints have also been investigated. Lee et al. [44] and Kim et al. [45] carried out experimental and numerical studies on welded plate to CHS chord X-joints with a nominal yield stress of 485 MPa and under in-plane bending in the brace. It is shown that the plate width to chord diameter ratio, chord diameter to wall thickness ratio and chord preload ratio affect applicability of design equations in the CIDECT design guide [14], and modified strength equations were proposed for the X-joints. Qu et al. [46, 47] conducted tests and finite element analysis on unstiffened and stiffened tube-gusset plate to CHS chord K-joints with a nominal yield stress of 690 MPa. Strength equations were proposed for the K-joints.

3.4. Remarks and research needs

The definition of joint strength is crucial for direct and objective comparison with the design codes and guides [9-17], which adopt different deformation limits as described in Section 2.1. It is noted that the joint strength in Cheng and Becque [33] was defined as the chord side wall buckling load, and the maximum load was taken as the joint strength in Feldmann et al. [38]. Havula et al. [37] determined the joint moment resistance as the intersection of the two tangent lines corresponding to initial and hardening stiffness in the moment-rotation curves. The definition of joint strength adopted by the CIDECT design guides [14, 15] i.e. lower of the maximum load and the load at the ultimate deformation limit was employed in other investigations [32, 34-36, 39-47]. In addition, the strength equations in the design codes and guides [9-17], in general, already include material and joint partial factors or joint resistance factors. It is therefore important to compare the joint strength obtained from tests and numerical simulations with the nominal strength calculated from the nominal strength equations on which the design codes and guides [9-17] are based, in order to allow for objective comparison.

The aforementioned investigations [32-47] indicate that applicability of design rules in EN 1993-1-8 [12] and the CIDECT design guides [14, 15] for different HSS welded hollow section joints depends on the loading type, failure mode, steel yield stress, geometric parameters, chord preload ratio, weld type and weld size. However, the current research on the HSS welded joints is mostly focused on axially loaded welded uniplanar RHS T-, X-, K- and N-joints, and welded CHS X-joints as well as welded plate to CHS chord X- and K-joint. Experimental, numerical and theoretical investigations on other joint types e.g. welded uniplanar CHS T-, Y-, K- and N-joints, welded plate to RHS or CHS chord joints, multiplanar welded joints and reinforced welded joints are therefore needed. It is noted that failure modes of welded hollow section joints depend on the joint parameters and loading type e.g. axial compression, tension and bending in the braces. Therefore, structural behaviours and static strengths of the HSS welded joints with parameter ranges common in practice and subjected to different loading needs to be further examined for comprehensive evaluation of current design provisions and proposing appropriate design rules for the HSS welded joints.

The welding of HSS is vital. Brace members are directly welded to the chord in welded hollow section joints. The heat input of welding into base metals could lead to a phase transition in heat affected zones (HAZ) and thus result in changes in microstructures and corresponding material properties. Material properties of HAZ in HSS mainly depend on the steel material (e.g. quenching and tempering, or thermo-mechanical controlled processing steel), heat input, welding type (e.g. gas metal arc welding or laser welding) and cooling time from 800 to 500 °C ($t_{8/5}$), and strength reduction of HAZ in HSS could be significant if welding is not properly controlled [43]. It is thus highly desirable to investigate material properties of HAZ in HSS welded hollow section joints and to examine effects of HAZ on the static strength and stiffness of the joints. Furthermore, Feldmann et al. [38] found that the current Eurocode EN 1993-1-8 [12] gives unduly conservative throat thickness for HSS fillet welds which could significantly increase corresponding welding costs of the HSS welded joints, and the throat thickness could be further reduced. Welding guidance which aims to avoid excessive material softening in HAZ and allow optimised design for HSS fillet welds is therefore highly desirable, and related research is needed.

4. Research advances of HSS welded hollow section joints under fatigue loading

4.1. General

The hot spot stress method adopted by the CIDECT design guide No. 8 [29] described in Section 2.2 is for the high-cycle fatigue design of welded hollow section joints ($N_f \geq 10^4$). The corresponding design provisions were developed using test data mostly from the welded joints using normal strength steel. Applicability of such design rules for high strength steel counterparts therefore needs to be examined. Research on low-cycle fatigue performance of the HSS welded joints ($N_f < 10^4$) is also desirable for the application of HSS tubular structures in seismic regions due to lower ductility of HSS when compared with normal strength steel. Some recent investigations on the HSS welded joints under fatigue loading and research needs are discussed in the following subsections.

4.2. High-cycle fatigue

Research on high-cycle fatigue performance of HSS welded hollow section joints remains limited. Jiang et al. [48] conducted experimental tests on two built-up box T-joints using RQT-S690 steel with a nominal yield stress of 690 MPa. Residual stresses and SCF distributions at brace-chord intersection of the T-joints subjected to axial loading, in-plane bending and out-of-plane bending were investigated. It is found that the residual stress and SCF at the corner of brace-chord intersection are highest, and the SCF values obtained from tests are generally lower than those predicted by the CIDECT design guide No. 8 [29]. Chiew et al. [49] carried out tests on fatigue performance of built-up box T-joints in RQT-S690 steel. It is found that crack propagation behaviours of the HSS T-joints are similar to those of hot-finished normal strength steel counterparts, and the fatigue resistance of the HSS T-joints is higher than that predicted by the CIDECT design guide No. 8 [29]. Additionally, the influence of residual stress on the crack depth development and crack penetration rate is found to be minor. Karcher and Puthli [50] performed fatigue tests on unstiffened and stiffened RHS and CHS L-joints with yield stresses up to 800 MPa, and found that the fatigue resistance of the L-joints using higher steel grades is higher at lower nominal stress ranges. These research findings indicate that the high-cycle fatigue resistance of the HSS welded joints could be comparable or even higher when compared with normal strength steel counterparts.

4.3. Low-cycle fatigue

Investigations on low-cycle fatigue performance of HSS welded hollow section joints have also been carried out. Varelis et al. [51] conducted experimental tests and numerical analysis on CHS X-joints with a nominal yield stress of 590 MPa and subjected to out-of-plane cyclic loading. It is found that the X-joints failed by through-thickness cracking at the chord saddle, and the fatigue resistance of the X-joints is affected by weld type. Kim et al. [52] carried out experimental and finite element investigations on CHS T-joints with yield stresses of 464 and 584 MPa under in-plane cyclic loading. The failure mode is cracking at the chord crown. It is found that the maximum moment in the hysteresis curves is close to the static moment resistance predicted by the ANSI/AISC 360-10 [13]. Qian et al. [53] conducted tests and numerical studies on pre-notched CHS X-joints in S690 steel. Cyclic loading followed by a monotonic in-plane bending was applied. Through-thickness cracking at the pre-cracked chord crown occurred in tests. It is found that the level 2A assessment curve in BS7910 [54] produces unconservative prediction of the failure load resulting in the brittle fracture in tests while the level 3C curve can provide more accurate estimation of the failure load.

4.4. Remarks and research needs

Investigations on high-cycle fatigue performance of HSS welded hollow section joints are mainly focused on built-up box T-joints and welded RHS and CHS L-joints. Research on low-cycle fatigue performance of the HSS welded joints is limited to CHS X- and T-joints. Experimental and numerical studies on fatigue performance of other HSS welded hollow section joints e.g. welded uniplanar CHS and RHS X-, K- and N-joints, welded plate to RHS and CHS chord joints and multiplanar welded joints are needed. On the one hand, it is necessary to examine suitability of the SCF formula and fatigue strength curves in design codes and guides e.g. the CIDECT design guide No. 8 [29] for the HSS welded joints. This is because the design rules are essentially empirical which are developed mainly based on test date of normal strength steel welded hollow section joints. Studies on the hysteretic behaviour, strength, ductility and energy dissipation of the HSS welded joints, on the other hand, are also needed in order to facilitate the application of HSS tubular structures in seismic regions.

Welded hollow section joints subjected to fatigue loading usually fail by fracture at the brace-chord intersection region. Fracture of the welded joints under high-cycle fatigue loading is generally stress-driven because applied cyclic stresses are low and strain within the welded joints is mostly smaller than the yield strain. Therefore, the corresponding fatigue resistance could be determined by the S_{rhs}-N_f curves. The yield stress of HSS is higher, and thus the fatigue resistance of the HSS welded joints could be comparable or higher than that of normal strength steel counterparts under the same low cyclic stress, which is in line with the research findings reported by Chiew et al. [49] and Karcher and Puthli [50]. However, fracture of welded hollow section joints under low-cycle fatigue loading is governed by the plastic damage due to the applied periodic plastic loading and large plastic strain occurring at the brace-chord intersection. It is noted that steel fracture under low-cycle fatigue loading could be characterised by micro-structure deterioration e.g. micro-void nucleation, growth and coalescence and micro-crack initiation and propagation [55]. The elongation is usually lower and the yield ratio of yield to ultimate stresses is closer to unity for HSS when compared with normal strength steel. The lower material ductility of HSS may lead to premature fracture failure and thus reduced ductility and energy dissipation capacity in the HSS welded joints under low-cycle fatigue loading. It is desirable to examine fracture mechanisms of HSS and to propose fracture models for HSS, which could pave way for research on fracture of HSS members, connections and structures. Experimental tests and numerical analysis on the fracture behaviour and fatigue resistance of the HSS welded joints under low-cycle fatigue loading remain limited, and related research is needed.

5. Conclusions

This paper provides a review of recent research advances of HSS welded hollow section joints under static and fatigue loadings. The current design codes and guides for the static design of welded hollow section joints, including EN 1993-1-8, the CIDECT design guides No. 1 and 3, ANSI/AISC 360-10, ISO 14346, and API RP 2A WSD, and corresponding research background are described. The hot spot stress method adopted by the CIDECT design guide No. 8 for the fatigue design of welded hollow section joints is elaborated. Recent research advances of HSS welded hollow section joints under static and fatigue loadings are summarised, and further research work is discussed. The preliminary research results indicate that suitability of current static design rules for the HSS welded joints depends on the loading type, failure mode, steel yield stress, geometric parameters, chord preload ratio, and welding. High-cycle fatigue performance of the HSS welded joints is comparable or even higher when compared with the normal strength steel counterparts. More research is needed for comprehensive assessment of current design provisions and proposing appropriate design rules for HSS welded hollow section joints.

Acknowledgements

The authors appreciate the support from the Chinese National Engineering Research Centre for Steel Construction (Hong Kong Branch) at The Hong Kong Polytechnic University. The financial support from The Hong Kong Polytechnic University (PolyU:1-ZE50/G-YBUU) is also gratefully acknowledged. The first author is also grateful for the support given by the Research Grants Council of Hong Kong for the Hong Kong PhD Fellowship Scheme.

References

[1] R. Bjorhovde, Performance and Design Issues for High Strength Steel in Structures, Adv. Struct. Eng. 13 (3) (2010) 403–411.

[2] J.L. Ma, T.M. Chan, B. Young, Tests on high-strength steel hollow sections: a review, P. I. Civil Eng. – Str. B. 170(9) (2017) 621–630.

[3] K. Nishioka, K. Ichikawa, Progress in thermomechanical control of steel plates and their commercialization, Sci. Technol. Adv. Mat. 13(2) (2012) 023001.

[4] H. Ban, G. Shi, A review of research on high-strength steel structures, P. I. Civil Eng. –Str. B. 171(8) (2017) 625–641.

[5] J.L. Ma, T.M. Chan, B. Young, Material properties and residual stresses of cold-formed high strength steel hollow sections, J. Constr. Steel Res. 109 (2015) 152-165.

[6] G. Shi, X. Zhu, H. Ban, Material properties and partial factors for resistance of high-strength steels in China, J. Constr. Steel Res. 121 (2016) 65–79.

[7] J. Wang, S. Afshan, N. Schillo, M. Theofanous, M. Feldmann, L. Gardner, Material properties and compressive local buckling response of high strength steel square and rectangular hollow sections, Eng. Struct. 130 (2017) 297-315.

[8] H.C. Ho, X. Liu, K.F. Chung, A.Y. Elghazouli, M. Xiao, Hysteretic behaviour of high strength S690 steel materials under low cycle high strain tests, Eng. Struct. 165 (2018) 222-236.

[9] International Institute of Welding (IIW) Subcommission XV-E, IIW Doc. XV-491-81: Design recommendations for hollow section joints–predominantly statically loaded, 1st Ed., IIW, Lisbon, 1981.

[10] International Institute of Welding (IIW) Subcommission XV-E, IIW Doc. XV-701-89: Design recommendations for hollow section joints–predominantly statically loaded, 2nd Ed., IIW, Paris, 1989.

[11] International Institute of Welding (IIW) Subcommission XV-E, IIW Doc. XV-1329-09: Static Design Procedure for Welded Hollow Section Joints–Recommendations, 3rd Ed., IIW, Singapore, 2009.

[12] Eurocode 3 (EC3), Design of Steel Structures-Part 1–8: Design of Joints. European Committee for Standardization, EN 1993-1-8, CEN, Brussels, 2005.

[13] ANSI/AISC 360-10. Specification for structural steel buildings. American Institute of Steel Construction (AISC), Chicago, 2010.

[14] J. Wardenier, Y. Kurobane, J.A. Packer, G.J. van der Vegte, X.L. Zhao, Design Guide for Circular Hollow Section (CHS) Joints under Predominantly Static Loading, CIDECT, Verlag TUV Rheinland, Cologne, Germany, 2008.

[15] J.A. Packer, J. Wardenier, X.L. Zhao, G.J. van der Vegte, Y. Kurobane, Design Guide for Rectangular Hollow Section (RHS) Joints Under Predominantly Static Loading, CIDECT, Verlag TUV Rheinland, Cologne, Germany, 2009.

[16] ISO. Static design procedure for welded hollow-section joints-Recommendations. ISO/FDIS 14346: 2012(E), Geneva.

[17] American Petroleum Institute (API), Recommended practice for planning, designing and constructing fixed offshore platforms-working stress design, API Recommended Practice 2A WSD (RP 2A WSD), 22nd Ed., 2014 (Washington).

[18] J. Wardenier, Hollow sections in structural applications, 2nd Ed., CIDECT, Geneva, 2011.

[19] L.H. Lu, G.D. de Winkel, Y. Yu, J. Wardenier, Deformation limit for the ultimate strength of hollow section joints, Tubular Structures VI, Balkema, Melbourne 1994, pp. 341–347.

[20]D. Pecknold, P. Marshall, J. Bucknell, New API RP2A tubular joint strength design provisions, J. Energ. Resour. 129 (2007) 177–189.

[21]G.J. van der Vegte, J. Wardenier, X.L. Zhao, J.A. Packer, Evaluation of new CHS strength formulae to design strengths, Tubular Structures XII, CRC Press, London 2009, pp. 313–322.

[22]X.L. Zhao, J. Wardenier, J.A. Packer, G.V.D. Vegte, Current static design guidance for hollow-section joints, P. I. Civil Eng. –Str. B. 163(6) (2010) 361–373.

[23]J. Wardenier, Hollow Section Joints, Delft University Press, The Netherlands, 1982.

[24]EN 1993-1-12, Eurocode 3: Design of Steel Structures-Part 1–12: Additional Rules for the Extension of EN 1993 up to Steel Grades S700, European Committee for Standardization, EN 1993-1-12, CEN, Brussels, 2007.

[25]D.K. Liu, J. Wardenier, Effect of the Yield Strength on the Static Strength of Uniplanar K-Joints in RHS (Steel Grade S460, S355 and S235), IIW Doc. XV-E-04-293, 2004.

[26]Y. Kurobane, New Development and Practices in Tubular Joint Design, IIW Doc. XV-448-81 and IIW Doc. XIII-1004-81, 1981.

[27]C. Noordhoek, A. Verheul, R.J. Foeken, H.M. Bolt, P.J. Wicks, Static strength of high strength steel tubular joints, ECSC agreement number 7210-MC/602, 1996.

[28]International Institute of Welding (IIW) Subcommission XV-E: Recommended fatigue design procedure for welded hollow section joints, Part 1: Recommendations and Part 2: Commentary, IIW Docs. XV-1035-99/XIII-1804-99, 1999.

[29]X.L. Zhao, S. Herion, J.A. Packer, R. Puthli, G. Sedlacek, J. Wardenier, K. Weynand, A. van Wingerde, N. Yeomans, Design Guide for Circular and Rectangular Hollow Section Welded Joints under Fatigue Loading, CIDECT, Verlag TUV, Germany, 2001.

[30]P.W. Marshall, Design of welded tubular connections: basis and use of AWS code provisions, Elsevier, 1992.

[31]X. L. Zhao, L.W. Tong, New development in steel tubular joints, Adv. Struct. Eng. 14(4) (2011) 699–715.

[32]J. Becque, T. Wilkinson, The capacity of grade C450 cold-formed rectangular hollow section T and X connections: an experimental investigation, J. Constr. Steel Res. 133 (2017) 345–359.

[33]S.S. Cheng, J. Becque, A design methodology for sidewall failure of RHS truss X-joints accounting for compressive chord pre-load, Eng. Struct. 126 (2016) 689–702.

[34]M. Mohan, T. Wilkinson, FEA of T & X joints in Grade C450 steel, Tubular Structures XIV, CRC Press, London 2012, pp. 185–194.

[35]M. Mohan, T. Wilkinson, Finite element simulations of 450 grade cold-formed K and N joints, Tubular Structures XV, CRC Press, Brazil 2015, pp. 449–456.

[36]J.H. Kim, Experimental and analytical study of RHS X-Joints under axial compression, Master Thesis, Seoul National University, 2018.

[37]J. Havula, M. Garifullin, M. Heinisuo, K. Mela, S. Pajunen, Moment-rotation behavior of welded tubular high strength steel T joint, Eng. Struct. 172 (2018) 523–537.

[38]M. Feldmann, N. Schillo, S. Schaffrath, K. Virdi, T. Björk, N. Tuominen, M. Veljkovic, M. Pavlovic, P. Manoleas, M. Heinisuo, K. Mela, P. Ongelin, I. Valkonen, J. Minkkinen, J. Erkkilä, E. Pétursson, M. Clarin, A. Seyr, L. Horváth, B. Kövesdi, P. Turán, B. Somodi, Rules on high strength steel, Luxembourg, Publications Office of the European Union, 2016.

[39]M. Pandey, B. Young, High strength steel tubular X-joints-an experimental insight under axial compression, Tubular Structures XV, CRC Press, Melbourne 2017, pp. 223–230.

[40]R. Puthli, O. Bucak, S. Herion, O. Fleischer, A. Fischl, O. Josat, Adaptation and extension of the valid design formulae for joints made of high-strength steels up to S690 for cold-formed and hot-rolled sections, CIDECT Report 5BT-7/10 (Draft Final Report), CIDECT, Germany, 2011.

[41]C.H. Lee, S.H. Kim, D.H. Chung, D.K. Kim, J.W. Kim, Experimental and numerical study of cold-formed high-strength steel CHS X-joints, J. Struct. Eng. 143 (8) (2017), 04017077.

[42]X.Y. Lan, T.M. Chan, B. Young, Static strength of high strength steel CHS X-joints under axial compression, J. Constr. Steel Res. 138 (2017) 369–379.

[43]X.Y. Lan, T.M. Chan, B. Young, Structural behaviour and design of chord plastification in high strength steel CHS X-joints, Constr. Build. Mater. 191 (2018), 1252-1267.

[44]S.H. Lee, K.J. Shin, H.D. Lee, W.B. Kim, J.G. Yang, Behavior of plate-to-circular hollow section joints of 600 MPa high-strength steel, Int. J. Steel Struct. 12(4) (2012) 473-482.

[45]W.B. Kim, K.J. Shin, H.D. Lee, S.H. Lee, Strength equations of longitudinal plate-to-circular hollow section (CHS) joints, Int. J. Steel Struct. 15(2) (2015) 499–505.

[46]S. Qu, X. Wu, Q. Sun, Experimental study and theoretical analysis on the ultimate strength of high-strength-steel tubular K-Joints, Thin Wall. Struct. 123 (2018) 244–254.

[47]S.Z. Qu, X.H. Wu, Q. Sun, Experimental and numerical study on ultimate behaviour of high-strength steel tubular K-joints with external annular steel plates on chord circumference, Eng. Struct. 165 (2018) 457–470.

[48]J. Jiang, C.K. Lee, S.P. Chiew, Residual stress and stress concentration effect of high strength steel built-up box T-joints, J. Constr. Steel Res. 105 (2015) 164–173.

[49]S.P. Chiew, M.S. Zhao, C.K. Lee, Fatigue performance of high strength steel built-up box T-joints, J. Constr. Steel Res. 106 (2015) 296–310.

[50]D. Karcher, R. Puthli, Design recommendations for stiffened and unstiffened L-joints made of CHS and RHS under fatigue loading, 11th ISOPE Conference, International Society of Offshore and Polar Engineers, Stavanger 2001, pp. 51–58.

[51]G.E. Varelis, S.A. Karamanos, Structural performance of TS590 high-strength steel welded tubular joints under extreme bending loading, Tubular Structures XIV, CRC Press, London 2012, pp. 211–218.

[52]J.W. Kim, S.S. Kim, M.J. Lee, J.G. Yang, Vierendeel joints in the circular hollow sections of high strength steel subjected to brace moment and chord compressive loadings, Int. J. Steel Struct. 12(4) (2012) 579-587.

[53]X. Qian, Y. Li, Z. Ou, Ductile tearing assessment of high-strength steel X-joints under in-plane bending, Eng. Fail. Anal. 28 (2013) 176-191.

[54]British Standards. Guide to methods for assessing the acceptability of flaws in metallic structures, BS7910:2005.

[55]L. Xue, A unified expression for low cycle fatigue and extremely low cycle fatigue and its implication for monotonic loading, Int. J. Fatigue 30(10-11) (2008) 1691-1698.

(a) Landmark Tower, Yokohama (600 MPa) [4]

(b) Lotte World Tower, Seoul (800 MPa) [4]

(c) Millau Bridge, Millau–Creissels (460 MPa) [4]

(d) Tokyo Gate Bridge, Tokyo (500, 700 MPa) [5]

Fig. 1. Engineering applications of high strength steel in buildings and bridges.

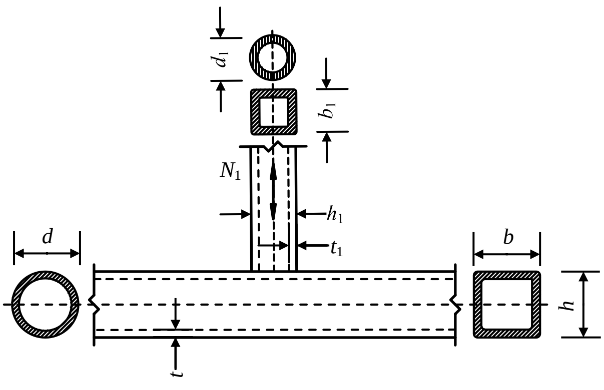

(a) T-joints

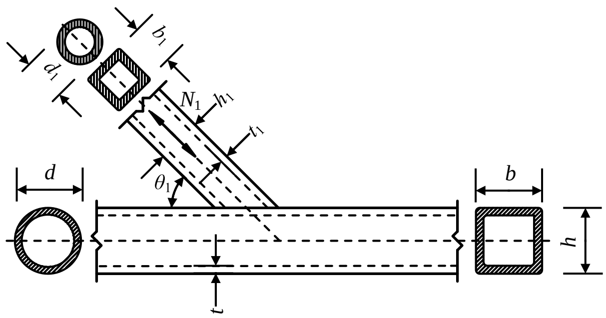

(b) Y-joints

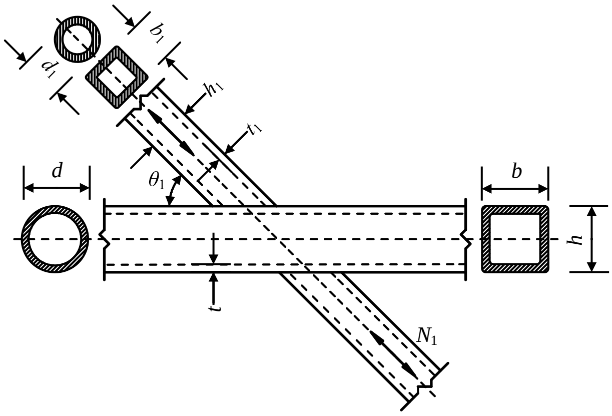

(c) X-joints

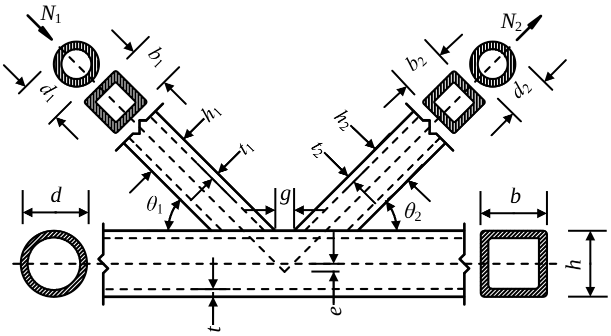

(d) Gap K-joints

Fig. 2. Examples of welded hollow section joints.

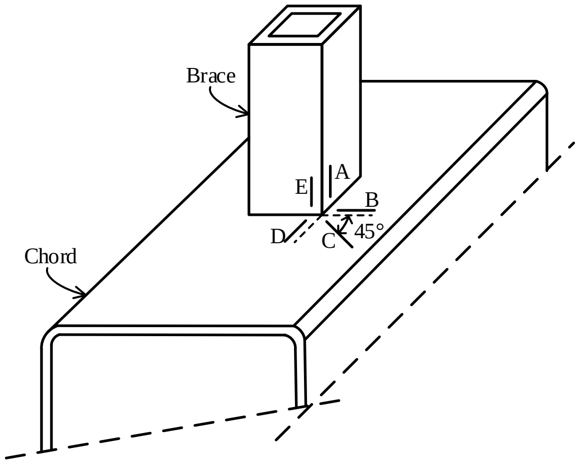

Fig. 3. Hot spot locations for RHS X- and T-joints.

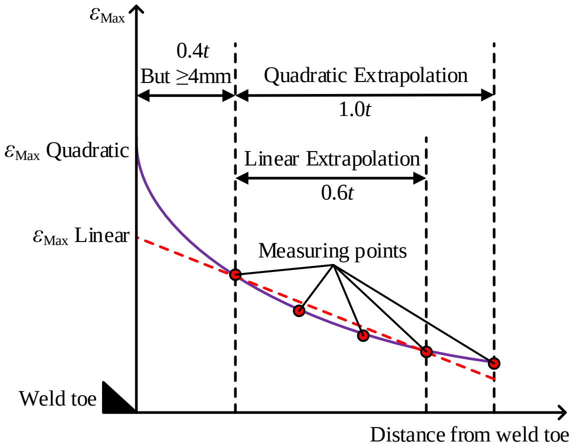

Fig. 4. Extrapolation region and method for hot spot stress method.